



Faster Growth Enhances Low Carbon Fuel and Chemical Production Through Gas Fermentation

Lorena Azevedo de Lima¹, Henri Ingelman¹, Kush Brahmhatt^{1†}, Kristina Reinmets¹, Craig Barry², Audrey Harris³, Esteban Marcellin², Michael Köpke³ and Kaspar Valgepea^{1*}

¹ERA Chair in Gas Fermentation Technologies, Institute of Technology, University of Tartu, Tartu, Estonia, ²Australian Institute for Bioengineering and Nanotechnology (AIBN), The University of Queensland, St. Lucia, QLD, Australia, ³LanzaTech Inc., Skokie, IL, United States

OPEN ACCESS

Edited by:

Fu-Li Li,

Qingdao Institute of Bioenergy and Bioprocess Technology (CAS), China

Reviewed by:

Christian Kennes,

University of A Coruña, Spain

Yang Gu,

Center for Excellence in Molecular Plant Sciences (CAS), China

*Correspondence:

Kaspar Valgepea

kaspar.valgepea@ut.ee

†Present address:

Tallinn University of Technology,

Tallinn, Estonia

Specialty section:

This article was submitted to Bioprocess Engineering, a section of the journal Frontiers in Bioengineering and Biotechnology

Received: 19 February 2022

Accepted: 14 March 2022

Published: 12 April 2022

Citation:

de Lima LA, Ingelman H, Brahmhatt K, Reinmets K, Barry C, Harris A, Marcellin E, Köpke M and Valgepea K (2022) Faster Growth Enhances Low Carbon Fuel and Chemical Production Through Gas Fermentation. *Front. Bioeng. Biotechnol.* 10:879578. doi: 10.3389/fbioe.2022.879578

Gas fermentation offers both fossil carbon-free sustainable production of fuels and chemicals and recycling of gaseous and solid waste using gas-fermenting microbes. Bioprocess development, systems-level analysis of biocatalyst metabolism, and engineering of cell factories are advancing the widespread deployment of the commercialised technology. Acetogens are particularly attractive biocatalysts but effects of the key physiological parameter—specific growth rate (μ)—on acetogen metabolism and the gas fermentation bioprocess have not been established yet. Here, we investigate the μ -dependent bioprocess performance of the model-acetogen *Clostridium autoethanogenum* in CO and syngas (CO + CO₂+H₂) grown chemostat cultures and assess systems-level metabolic responses using gas analysis, metabolomics, transcriptomics, and metabolic modelling. We were able to obtain steady-states up to $\mu \sim 2.8 \text{ day}^{-1}$ ($\sim 0.12 \text{ h}^{-1}$) and show that faster growth supports both higher yields and productivities for reduced by-products ethanol and 2,3-butanediol. Transcriptomics data revealed differential expression of 1,337 genes with increasing μ and suggest that *C. autoethanogenum* uses transcriptional regulation to a large extent for facilitating faster growth. Metabolic modelling showed significantly increased fluxes for faster growing cells that were, however, not accompanied by gene expression changes in key catabolic pathways for CO and H₂ metabolism. Cells thus seem to maintain sufficient “baseline” gene expression to rapidly respond to CO and H₂ availability without delays to kick-start metabolism. Our work advances understanding of transcriptional regulation in acetogens and shows that faster growth of the biocatalyst improves the gas fermentation bioprocess.

Keywords: gas fermentation, acetogen, *Clostridium autoethanogenum*, carbon recycling, metabolomics, transcriptomics, genome-scale metabolic modelling, chemostat

INTRODUCTION

Climate change is causing alarming detrimental degradation to the environment. The world thus needs to decarbonize energy production (e.g., solar, wind) and move away from producing fuels and chemicals from fossil carbon. Furthermore, improved recycling of solid waste (e.g., municipal solid waste [MSW], plastic waste) is becoming increasingly important to maintain biosustainability. Gas fermentation offers a sustainable route for the production of renewable chemicals and fuels by recycling gaseous one-carbon

(C1) waste feedstocks using gas-fermenting organisms [e.g., industrial waste gases, syngas from gasified MSW or biomass ($\text{CO} + \text{H}_2 + \text{CO}_2$)] (Liew et al., 2016; Redl et al., 2017; Fackler et al., 2021; Pavan et al., 2022). Acetogen bacteria are particularly attractive for gas fermentation as they can accept gas (CO) as their sole energy and carbon source (Wood 1991) and use the most efficient pathway to fix CO_2 (Drake et al., 2006; Fast and Papoutsakis 2012; Cotton et al., 2018), the Wood-Ljungdahl pathway (WLP) (Wood 1991; Ragsdale and Pierce, 2008). Acetogens can natively convert carbon into acetic acid, ethanol, or 2,3-butanediol among other products while metabolic engineering for expanding their product spectrum is advancing rapidly (Köpke and Simpson 2020; Bourgade et al., 2021; Fackler et al., 2021; Pavan et al., 2022). Notably, the acetogen *Clostridium autoethanogenum* is used as a commercial-scale gas fermentation cell factory (Köpke and Simpson, 2020).

A better understanding of acetogen metabolism and the gas fermentation bioprocess can contribute to the widespread deployment of the technology. Recent systems-level studies have improved the much-needed quantitative understanding of the energy-limited metabolism of acetogens (Schuchmann and Müller, 2014; Molitor et al., 2017) to advance their rational metabolic engineering. For example, regulatory principles behind metabolic shifts in carbon, energy, and redox balances (Richter et al., 2016; Valgepea et al., 2017a, 2018; Mahamkali et al., 2020), metabolic robustness (Mahamkali et al., 2020), and transcriptional and translational regulation (Song et al., 2017; Al-bassam et al., 2018; Song et al., 2018; Lemgruber et al., 2019; Shin et al., 2021) have been quantified. At the same time, understanding of the gas fermentation bioprocess has also improved with the characterisation of the effects of gas-liquid mass transfer, feed gas and media composition, pH shifts, and mixed cultures on the biocatalyst and fermentation performance, e.g. gas uptake, biomass level, product profile, yields, and rates (Cotter et al., 2009; Abubackar et al., 2012; Abubackar et al., 2015; Valgepea et al., 2017b, 2018; Esquivel-Elizondo et al., 2017; Diender et al., 2019; Park et al., 2019; Heffernan et al., 2020). However, the effects of the specific growth rate (μ) of the cells on acetogen metabolism and on the gas fermentation bioprocess have not yet been established.

Characterisation of μ -dependent acetogen growth is important for three reasons. Firstly, it could reveal important insights into the energy-limited metabolism of acetogens (Schuchmann and Müller, 2014; Molitor et al., 2017) as faster growth demands more energy. Secondly, studies of the impact of μ on cell metabolism in other microorganisms have, for instance, revealed profound effects on product distribution and energy balance (Van Hoek et al., 1998; Valgepea et al., 2010), transcript and protein expression (Ishii et al., 2007; Valgepea et al., 2010, 2013; Peebo et al., 2015; Hackett et al., 2016), and stress responses (Regenberg et al., 2006). Thirdly, μ of the cell culture is an important bioprocess parameter affecting metabolic activity of cells, process rates, and economics (Lipson 2015). This is especially relevant for acetogen gas fermentation as the process is operated as a continuous culture at industrial-scale (Köpke and Simpson, 2020; Fackler et al., 2021). Thus, the selection of culture

dilution rate (i.e., μ at steady-state) is critical for optimal bioprocess performance (e.g. titre, rate, yield).

In this work, we investigate the μ -dependent bioprocess performance of the acetogen *C. autoethanogenum* in CO- and syngas-grown chemostat cultures and assess systems-level metabolic responses using gas analysis, metabolomics, transcriptomics, and metabolic modelling. We obtained steady-states up to $\mu \sim 2.8 \text{ day}^{-1}$ ($\sim 0.12 \text{ h}^{-1}$) and show that faster growth supports both higher yields and productivities for reduced by-products ethanol and 2,3-butanediol (2,3-BDO), thereby benefitting the gas fermentation bioprocess. Transcriptomics data suggest that *C. autoethanogenum* uses transcriptional regulation to a large extent for facilitating faster growth and emphasise the need for mapping genotype-phenotype links and improving gene annotations in acetogens for advancing understanding of metabolism and engineering of cell factories.

MATERIAL AND METHODS

Bacterial Strain, Growth Medium, and Continuous Culture Conditions

A derivative of *Clostridium autoethanogenum* DSM 10061 strain—DSM 23693—deposited in the German Collection of Microorganisms and Cell Cultures (DSMZ) was used in all experiments and stored as a glycerol stock at -80°C . Cells were grown either on CO (60% CO and 40% Ar; AS Eesti AGA) or syngas (50% CO, 20% H_2 , 20% CO_2 , and 10% Ar; AS Eesti AGA) in a chemically defined medium without yeast extract described before (Valgepea et al., 2017a). Cells were grown under strictly anaerobic conditions at 37°C and at pH 5 maintained by 5M NH_4OH . Chemostat continuous cultures were performed in 1.4 L Multifors bioreactors (Infors AG) at a working volume of 750 mL connected to a Hiden HPR-20-QIC mass spectrometer (Hiden Analytical) for online high-resolution off-gas analysis. The system was equipped with peristaltic pumps; mass flow controllers (MFCs); pH, oxidation-reduction potential (ORP), and temperature sensors. Antifoam (435530; Sigma-Aldrich) was continuously added to the bioreactor at a rate of 10 $\mu\text{L}/\text{h}$ to avoid foaming. Chemostat cultures were run at three dilution rates: ~ 1.0 , ~ 2.0 , and $\sim 2.8 \text{ day}^{-1}$ ($\mu \sim 0.04$, 0.08, and 0.12 h^{-1} , respectively) with variable gas-liquid mass transfer conditions (gas flow rate and agitation) to maintain similar steady-state biomass concentrations (Table 1). All steady-state results reported here were collected after optical density (OD), gas uptake, and production rates had been stable for at least 3–5 working volumes.

Biomass Concentration Analysis

Biomass concentration in gram of dry cell weight per litre of broth (gDCW/L) was determined by measuring the OD of the culture at 600 nm after the correlation coefficient (K) between culture OD and DCW was established at 0.23, using the methodology described in Peebo et al., 2014.

TABLE 1 | Variable operational parameters of 23 steady-state chemostat cultures of *C. autoethanogenum*.

Feed gas	Gas flow rate (mL/min)	Agitation (RPM)	μ (day ⁻¹)	Biomass concentration (gDCW/L)	Number of bioreplicates
CO	50	690	1.02 ± 0.01	1.58 ± 0.06	4
	72	815	2.03 ± 0.06	1.65 ± 0.01	3
	72	1175	2.79 ± 0.03	1.65 ± 0.02	3
Syngas	50	675	1.01 ± 0.02	1.59 ± 0.03	6
	72	800	2.01 ± 0.07	1.57 ± 0.08	3
	72	1160	2.79 ± 0.07	1.43 ± 0.03	4

μ , specific growth rate; gDCW, gram of dry cell weight.

Data are average ± standard deviation between bioreplicates.

Extracellular Metabolome Analysis

Analysis of exo-metabolome was performed using filtered broth samples stored at -20°C until analysis. Organic acids and alcohols were analysed by HPLC (Shimadzu Prominence-I LC-2030 plus system) using a Rezex™ ROA-Organic Acids H⁺ (8%) 300 × 7.8 mm column (00H-0138-K0; Phenomenex) and a guard column (03B-0138-K0; Phenomenex). Twenty microlitres of the sample were injected using an auto-sampler and eluted isocratically with 0.5 mM H₂SO₄ at 0.6 mL/min for 30 min at 45°C. Compounds were detected by a refractive index detector (RID-20A; Shimadzu) and identified and quantified using relevant standards using the software LabSolution (Shimadzu). We note that cells produced 2R,3R-butenediol.

Bioreactor Off-Gas Analysis

Bioreactor off-gas analysis for determination of specific gas uptake (CO and H₂) and production rates (CO₂, ethanol) (mmol/gDCW/h) has been described before (Valgepea et al., 2017a). The Faraday Cup detector monitored the intensities of H₂, CO, ethanol, H₂S, Ar, and CO₂ at 2, 14, 31, 34, 40, and 44 amu, respectively. Argon was used as the inert gas component in the feed gases instead of nitrogen as the latter interferes with the mass-spectrometer signal for CO.

Carbon Balance Analysis

Carbon recoveries and balances were determined as described before (Valgepea et al., 2017a). Briefly, carbon balancing of substrate carbon (CO, cysteine) between growth products (acetate, ethanol, 2,3-BDO, CO₂, biomass) was calculated as C-mol fraction of each product from total C-mol carbon uptake. Carbon recoveries were calculated as the fraction of summed C-mol products from total C-mol substrates. Ethanol stripping and the total soluble CO₂ fraction in culture broth were also taken into account to achieve more accurate carbon balancing.

Transcriptome Analysis

Transcriptome analysis of 20 chemostat cultures was conducted using RNA sequencing (two and one bio-replicate of syngas cultures at ~1 and ~2.8 day⁻¹, respectively, indicated in Table 1 were excluded due to experimental constraints). Ten millilitres of culture were pelleted by immediate centrifugation (5,000 × g for 3 min at 4°C) and resuspended in 5 mL of RNAlater

(76106; Qiagen). Samples were stored at 4°C overnight, centrifuged (4,000 × g for 10 min at 4°C), and pellets stored at -80°C until RNA extraction.

Thawed cell pellets were resuspended in 800 μL of RLT buffer (74104; Qiagen) containing 10 μL of β-mercaptoethanol and lysed with acid-washed glass beads (G4649; Merck) using the Precellys® 24 instrument with liquid nitrogen cooling (Bertin Technologies). Total RNA was extracted using the RNeasy mini kit (74104, Qiagen) with off-column TURBO™ DNase treatment (AM2239; Invitrogen), followed by purification and enrichment using the RNA Clean and Concentrator™ kit (R1018, Zymo). The efficiency of the total RNA purification and DNA removal was verified using the NanoDrop™ 1,000 instrument (Thermo Scientific) and the quality of RNA extracts was checked using the TapeStation 2200 equipment (Agilent Technologies). Total RNA concentration was determined using the Qubit 2.0 instrument (Q32866; Invitrogen). Next, ribosomal RNA (rRNA) was removed using the QIAseq FastSelect -5S/16S/23S Kit (335925; Qiagen) and stranded mRNA libraries were prepared using the QIAseq Stranded RNA Lib Kit (180743; Qiagen). RNA sequencing was performed using the NextSeq MID150 sequencing kit (20024904; Illumina) on the NextSeq500 sequencer (Illumina) with 2 × 75 bp paired-end dual indexed (2 × 8 bp) reads, which produced eight fastq files per sample (160 files in total).

RNA Sequencing Data Analysis

The R-scripts used for the analysis of RNA sequencing data after read trimming includes complete details of the methodology and can be downloaded as **Supplementary Files S1, S2**.

Mapping and Assignment of Genome Features From RNA Sequencing Raw Data

The quality of raw NextSeq reads was verified using MultiQC (Ewels et al., 2016) and adapter sequences were trimmed using the Cutadapt Python package (version 2.10; Martin 2011) allowing a minimum read length of 35 nucleotides. The resulting high-quality paired-end reads were mapped to the NCBI reference genome NC_022592.1 (Brown et al., 2014) using the align function within Rsubread package (version 2.4.2; Liao et al., 2019). Thereafter, four .bam files per sample were merged using Samtools (version 1.10; Li et al., 2009) and genomic features were assigned using the featureCounts

functions within Rsubread. Samples had 5.6–9.3 million reads with an average mapping rate of 99% and this generated 4.3–6.4 million feature counts across samples (**Supplementary Table S1**). The NCBI annotation NC_022592.1 of the *C. autoethanogenum* sequence (Brown et al., 2014) was used as the annotation genome, including only coding (CDS) and non-coding (ncRNA) sequences. Additionally, CAETHG_RS07860 was removed from the annotation and replaced with the carbon monoxide dehydrogenase genes with initial IDs of CAETHG_1620 and 1621 (Brown et al., 2014) which were given the IDs CAETHG_RS07861 and RS07862, respectively.

Determination of Transcript Abundances and Differentially Expressed Genes

Transcript abundances and DEGs were determined as described before (Valgepea et al., 2017a). In short, raw library sizes were normalised and transcript abundances in reads per kilobase of transcript per million mapped reads (RPKM) were estimated from feature counts and gene lengths using edgeR (version 3.32.1; Robinson et al., 2010). Transcripts with abundances >10 RPKMs in at least two samples were subject to differential expression analysis using limma (version 3.46.0; Ritchie et al., 2015) between bio-replicate cultures of different μ values within one gas mixture (i.e., gas mixes at same μ were not compared). DEGs were determined by fold-change > 1.5 and q-value < 0.05 after false discovery rate (FDR) correction (Benjamini and Hochberg, 1995). Transcript abundances and DEGs are presented in **Supplementary Tables S2–S5**, respectively. Proposed gene names were obtained from Valgepea et al., 2021. RNA sequencing data (NextSeq) has been deposited in the NCBI Gene Expression Omnibus repository under accession number GSE196640.

Functional Data Analysis

Mapping of gene IDs to Cluster of Orthologous Groups (COGs) was performed using the eggNOG 5.0 database (Huerta-Cepas et al., 2019) that resulted in COG assignment for 1,190 genes (**Supplementary Table S6**). The Gene Ontology (GO) terms list was assembled using Pannzer2 (Törönen et al., 2018), InterProScan5 (Jones et al., 2014), and eggNOG 5.0 databases that resulted in GO term assignment for 3,001 genes (**Supplementary Table S7**). Clustering of transcript expression profiles across μ values and gas mixes in **Figure 5B** was performed and visualised using the dendextend (version 1.14.0; Galili 2015) and ComplexHeatmap (version 2.10.0; Gu et al., 2016) packages in R using Ward's ward. D2 hierarchical clustering algorithm. Six clusters were identified based on the sharp decline of the dendrogram height parameter for other clusters. Functional enrichment analysis of GO terms was performed using the topGO package in R (version 2.40.0; Alexa and Rahnenfuhrer, 2020) and a custom-made script (**Supplementary File S2**) with significant enrichment indicated by q-Fisher < 0.05 for FDR-corrected Fisher's exact test. The 245 genes that quantitatively showed the same expression trend with increasing μ on both gas mixes (**Figure 5C**) were determined by a *t*-test (*p*-value < 0.05) between the slopes of linear regression of gene expression change on the two gas mixes for genes that

showed a continuously increasing or decreasing differential expression (i.e., DEGs for both $\mu = 2.0$ vs. 1.0 and 2.8 vs. 2.0 day⁻¹) with increasing μ on both gases.

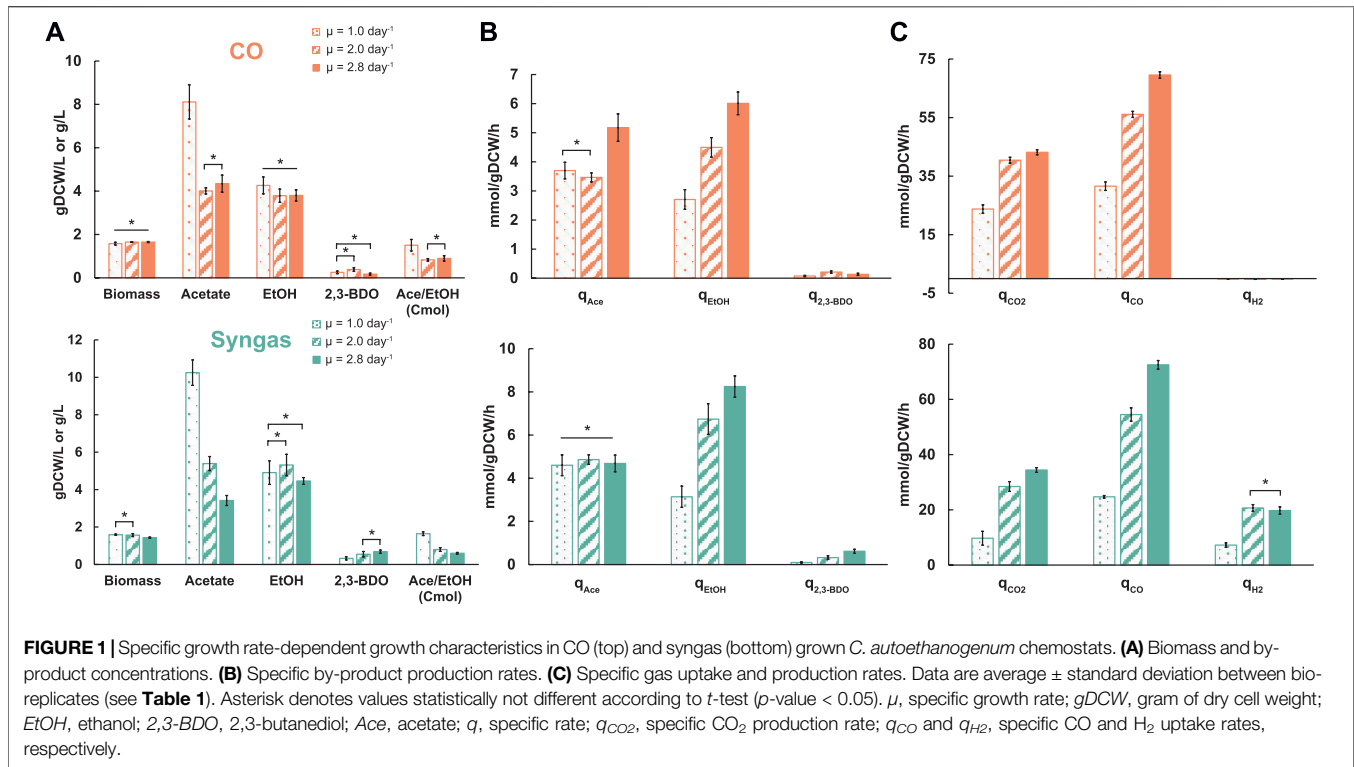
Genome-Scale Metabolic Modelling

Metabolic model simulations were performed using the genome-scale model iCLAU786 of *C. autoethanogenum* (Valgepea et al., 2018) and flux balance analysis (FBA) (Orth et al., 2010) as specified in Valgepea et al. (2018). We used the COBRA Toolbox (Schellenberger et al., 2011) as the programming platform for FBA with Gurobi (Gurobi Optimization Inc.) as the linear programming solver. We note three characteristics of our model network: a) methylene-THF reductase is NADH-specific and reducing ferredoxin (Fd); b) membrane-bound Fd-NAD⁺ oxidoreductase Rnf complex translocates 2H⁺/reduced Fd and c) 4H⁺/ATP stoichiometry for the ATP synthase. We estimated intracellular metabolic flux rates (SIM1–23 in **Supplementary Tables S8, S9**) using experimentally measured constraints [e.g., μ , substrate consumption and product production rates (CO, H₂, CO₂, cysteine, acetate, ethanol, and 2,3-BDO)] and maximisation of ATP dissipation as the objective function in FBA. Prediction of optimal growth phenotypes for μ and products (SIM24–46) was performed using experimental substrate uptake rates (CO, cysteine, and H₂ for syngas), the ATP dissipation flux calculated above, and maximisation of biomass yield as the objective function. Accuracy of growth phenotype prediction was improved (SIM47–59) by additionally zeroing CO₂ reduction with the redox-consuming FdhA activity (reaction rxn00103_c0) and fixing the ratio between H₂ utilisation for direct CO₂ reduction (reaction rxn08518_c0), and Fd_{red} and NADPH generation (reaction leq000001) by the HytA-E/FdhA complex at a value corresponding to the respective experiment's q_{H2}/q_{CO} ratio (see Valgepea et al., 2018 for details). Simulation results identified as SIMx (e.g., SIM1) in the text are reported in **Supplementary Tables S8, S9**, while the SBML model file of iCLAU786 is supplied in Valgepea et al. (2018).

RESULTS

Steady-State Gas-Fermenting Chemostat Cultures of *Clostridium autoethanogenum*

We used continuous cultures for controlling the μ of cells as this allows to unequivocally quantify the effects of μ on cell growth compared to batch cultures where genetically modified strains (e.g., titratable substrate uptake) or variable culture parameters (e.g., growth media) need to be used to adjust μ of cells that might confound results (Adamberg et al., 2015). Here, the acetogen *Clostridium autoethanogenum* was grown in 23 chemostats where cells reached steady-states on CO or syngas (CO + CO₂+H₂) using a chemically defined medium in biological triplicates or quadruplicates at dilution rates ~1.0, ~2.0, and ~2.8 day⁻¹ (μ ~0.04, 0.08, and 0.12 h⁻¹, respectively) (**Table 1**). In addition to continuous quantification of gas uptake and production rates, cultures were sampled for extracellular metabolome and



transcriptome analysis. We also used genome-scale metabolic modelling to estimate intracellular flux rates.

Elevated Ethanol Productivity With Faster Growth

We adjusted gas-liquid mass transfer conditions (gas flow rate and agitation) between different dilution rates to maintain similar steady-state biomass concentrations ($\sim 1.6 \pm 0.1$ gDCW/L; average \pm standard deviation) (**Table 1**; **Figure 1A**) as it can affect acetogen carbon distribution (Valgepea et al., 2017a). We detected secretion of acetate, ethanol, and 2,3-BDO by the cells (**Figure 1A**). While specific acetate production rate (q_{Ace} ; mmol/gDCW/h) profiles with increasing μ varied between the two gases, specific ethanol production rates (q_{EtOH}) more than doubled on both gases (**Figure 1B**). This also means higher productivity (g/L/h) due to similar biomass levels. Increasing trends for specific 2,3-BDO production rates ($q_{2,3-BDO}$) were also seen with higher μ . Notably, faster growth led to molar acetate/ethanol ratios dropping from ~ 1.5 to 0.9 and 0.6 for CO and syngas, respectively, due to a strong decrease of acetate levels at similar ethanol values (**Figure 1A**). These trends are beneficial for an industrial ethanol production process as higher productivity is not comprised with lower selectivity.

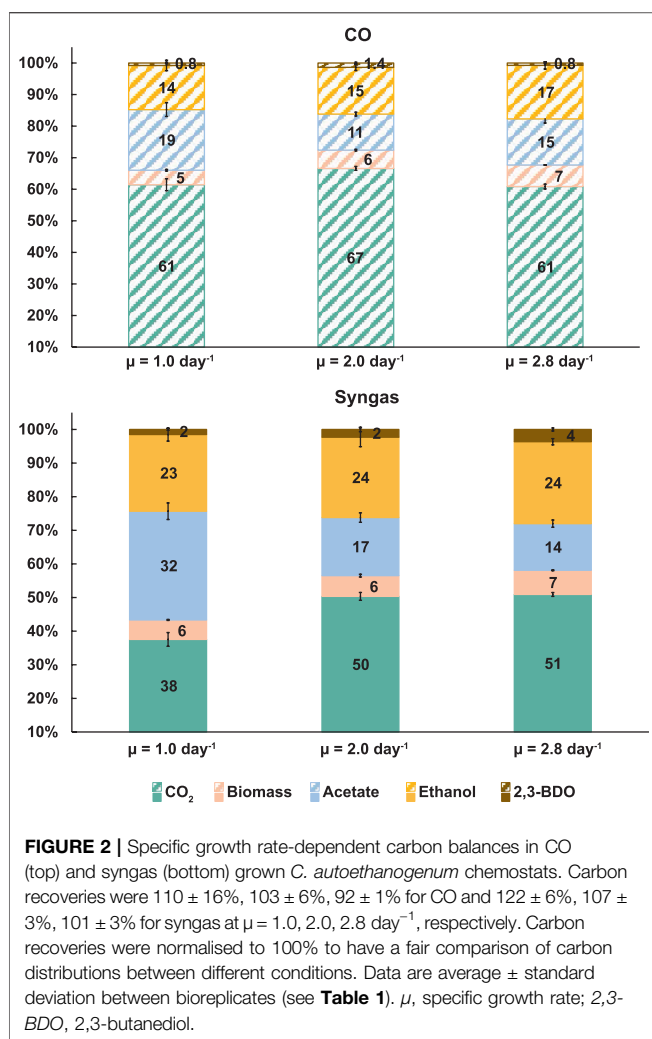
Gas Analysis Indicates Metabolic Rearrangements

CO limited our chemostats since we could maintain similar steady-state biomass concentrations across dilution rates by changing gas-

liquid mass transfer (**Table 1**). One could thus expect the specific CO uptake rate (q_{CO} ; mmol/gDCW/h) to increase proportionally with μ . We detected q_{CO} to increase ~ 2.2 - (32 ± 1 to 70 ± 1) and ~ 2.9 -fold (25 ± 1 to 73 ± 2) for CO and syngas cultures, respectively, with 2.8-fold faster growth (**Figure 1C**). The non-proportional change for CO cultures means a higher biomass yield (gDCW/mmol of CO consumed) at higher μ . As expected for CO-limited chemostats (Richter et al., 2013; Martin et al., 2015; Valgepea et al., 2018), simultaneous uptake of CO and H_2 were observed for syngas cultures (**Figure 1C**). Interestingly, while the specific H_2 uptake rate (q_{H_2} ; mmol/gDCW/h) increased ~ 2.9 -fold (7 ± 1 to 21 ± 1) between $\mu = 1.0$ and 2.0 day $^{-1}$ on syngas, no further change was seen with faster growth, despite gas-liquid mass transfer (gas flow rate and agitation) being increased with dilution rate. Specific CO_2 production rates (q_{CO_2} ; mmol/gDCW/h) increased ~ 1.8 - (24 ± 1 to 43 ± 1) and ~ 3.4 -fold (10 ± 2 to 34 ± 1) for the CO and syngas cultures, respectively (**Figure 1C**), indicating a strong effect of H_2 uptake on CO oxidation as seen before for *C. autoethanogenum* growing on various gas mixes (Valgepea et al., 2018).

Faster Growth Leads to Carbon Diversion Away From Acetate

Product ratios show the distribution of carbon between products but carbon balancing is necessary to quantify carbon flows from substrates to products (i.e. yields). Notably, carbon flux to acetate dropped with faster growth by 24% ($19.2 \pm 2.2\%$ to $14.6 \pm 1.3\%$) on CO and by 57% ($32.3 \pm 2.5\%$ to $13.9 \pm 1.1\%$) on syngas (**Figure 2**). While no clear μ -dependent trend for carbon flow to 2,3-BDO was detected on CO, cells diverted up to 141% more carbon into 2,3-BDO



in syngas cultures ($1.5 \pm 0.3\%$ to $3.6 \pm 0.4\%$). The aforementioned doubling of q_{EtOH} with faster growth (**Figure 1B**) was supported by up to $\sim 21\%$ elevated carbon flux to ethanol (**Figure 2**). These observations are not trivial as faster growth demands more energy while reduced products like ethanol and 2,3-BDO consume redox co-factors that acetogens could otherwise use for ATP generation (Schuchmann and Müller, 2014). In fact, cells were even able to channel more carbon into biomass formation simultaneously (increase of ~ 48 and $\sim 24\%$ for CO and syngas, respectively; **Figure 2**). The ~ 60 and $\sim 50\%$ losses of substrate carbon as CO₂ for the CO and syngas cultures, respectively, are close to theoretical stoichiometric and thermodynamic calculations for CO₂ dissipation with ethanol production from CO ($\sim 67\%$) or from a gas mix with a CO-to-H₂ ratio around two (50%) (Wilkins and Atiyeh, 2011; Molitor et al., 2016).

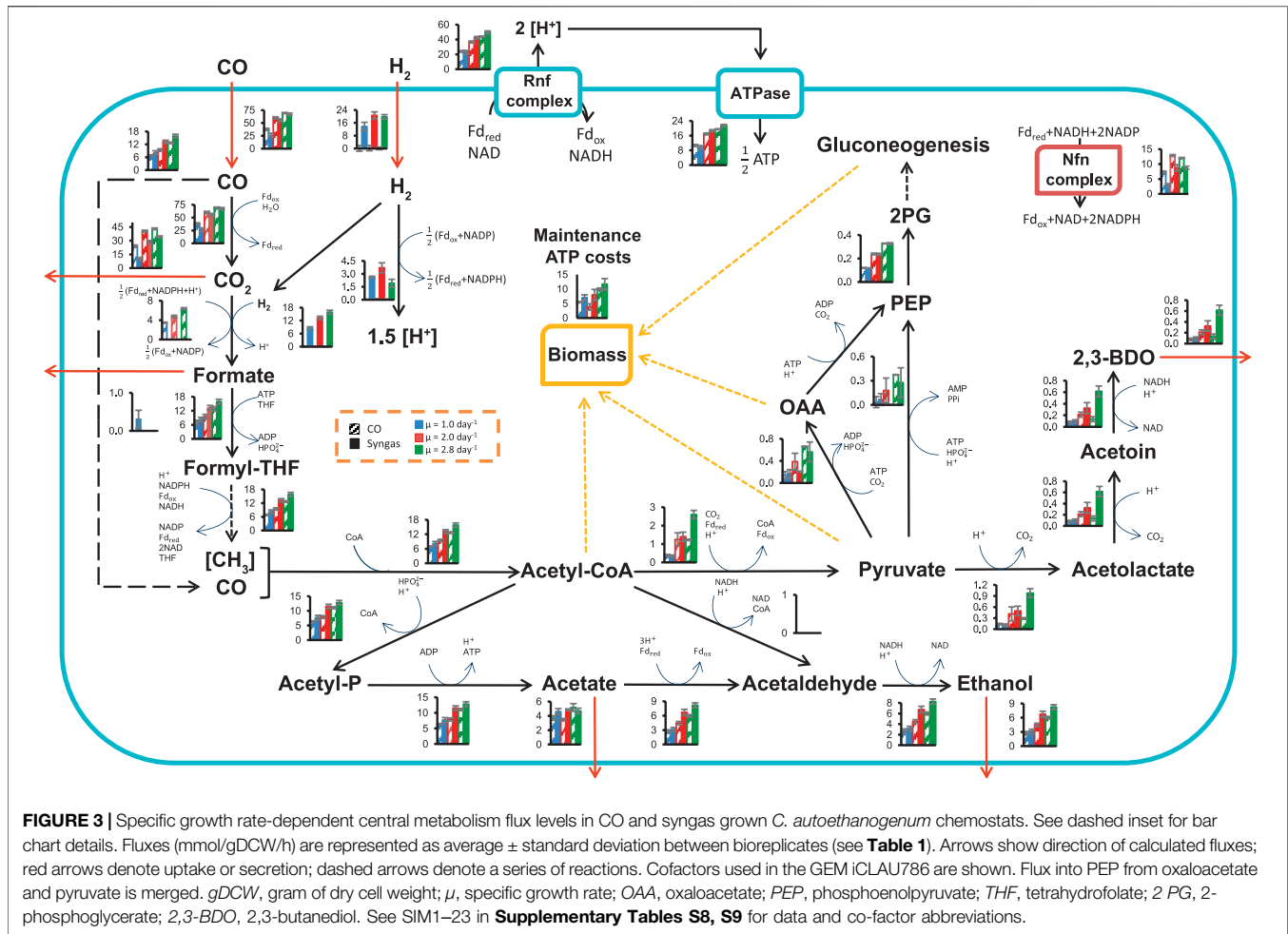
Analysis of Metabolic Fluxes Using a Genome-Scale Metabolic Model

We took advantage of the quantitative steady-state data collected above on carbon and redox flows entering and leaving the cells to

estimate intracellular metabolic fluxes using the genome-scale metabolic model (GEM) iCLAU786 of *C. autoethanogenum* (Valgepea et al., 2018) and flux balance analysis (FBA) (Orth et al., 2010). Steady-state intracellular flux patterns for our CO and syngas chemostats were estimated by constraining the GEM with experimental data (exchange rates and μ) and maximising ATP dissipation as the objective function in FBA (SIM1–23 in **Supplementary Tables S8, S9**).

Flux through the WLP was significantly increased as expected with faster growth, although less than the increase in CO uptake for syngas cultures as more of the fixed CO was oxidised and dissipated as CO₂ (**Figure 3; Supplementary Tables S8, S9**). Faster growth was also supported with elevated ATP production through the ATPase (by 82 and 125% on CO and syngas, respectively; **Figure 3; Supplementary Tables S8, S9**). Interestingly, the ratio between the ATP production fluxes of the ATPase and the acetate kinase (acetyl-P \rightarrow acetate) changed minimally (9% in average; **Supplementary Tables S8**), despite significantly altered product distributions (**Figure 2**). At the same time, maintenance ATP costs increased by 80 and 66% to 9.9 ± 0.5 and $11.7 \pm 1.9 \text{ mmol/gDCW/h}$ on CO and syngas, respectively (**Figure 3; Supplementary Tables S8, S9**). The average $\sim 30\%$ fraction of maintenance costs from total ATP production (**Supplementary Table S8**) is similar to previously studied autotrophic *C. autoethanogenum* cultures (Valgepea et al., 2017a, 2018). In addition to ATP, biomass synthesis during faster growth also demands an elevated supply of NADPH. Notably for *C. autoethanogenum*, extra NADPH was provided by increased flux through the Nfn transhydrogenase (by 66 and 190% to 12.0 ± 0.2 and $8.8 \pm 0.5 \text{ mmol/gDCW/h}$ on CO and syngas, respectively), and not by higher flux through the electron-bifurcating hydrogenase HytA-E complex on syngas (**Figure 3**). No increase in flux through HytA-E with faster growth on syngas suggested that production of the critical reducing power co-factor, reduced ferredoxin (Fd_{red}), was possibly supported by CO oxidation. Indeed, the model demonstrated an increase of the fraction of Fd_{red} generated by CO oxidation from $63 \pm 2\%$ to $74 \pm 1\%$ with increasing μ (**Supplementary Table S8**). As seen for previous CO + H₂ or CO₂+H₂-fermenting *C. autoethanogenum* steady-state cultures (Valgepea et al., 2017a, 2018; Heffernan et al., 2020), all the CO₂ in the WLP was reduced to formate directly using H₂ through the formate-H₂ lyase activity of the HytA-E/formate dehydrogenase (FdhA) complex (Wang et al., 2013). This saves valuable redox for the cells compared to growth on CO only and allows higher production of reduced products when H₂ is available (**Figure 2**). Regarding ethanol production, our simulations are consistent with the aforementioned *C. autoethanogenum* datasets and gene knockout experiments (Liew et al., 2017) showing that ethanol was synthesised using the aldehyde:Fd oxidoreductase (AOR) activity through acetate to couple it with ATP production (**Figure 3**).

GEMs can also be used for predicting growth phenotypes (O'Brien et al., 2015) and the accuracy of the model can be evaluated beforehand, for example, by comparing experimental product profiles with predicted ones if constraining only substrate uptake rates, maintenance ATP costs, and maximising biomass



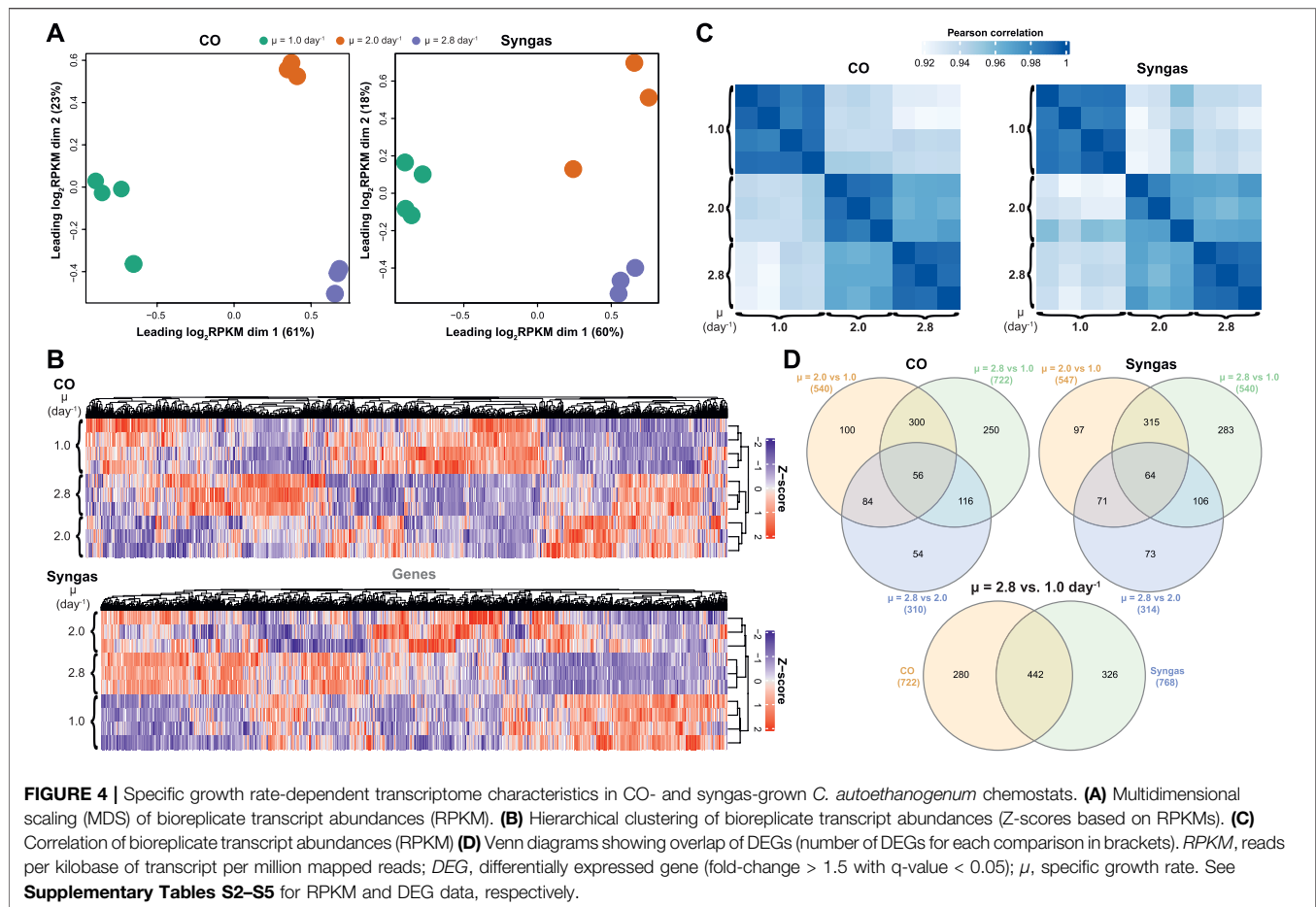
yield in FBA. We initially failed to predict ethanol and 2,3-BDO production (SIM24–46 in **Supplementary Tables S8, S9**), as seen before (Valgepea et al., 2017a, 2018). However, when additionally constraining the model by coupling carbon and redox metabolism from H_2 utilisation for syngas cultures (see Materials and Methods), predictions improved as ethanol production became on average 28% off from experimental values (SIM47–59 in **Supplementary Tables S8, S9**). Prediction of acetogen phenotypes can be further improved by considering thermodynamics and kinetics (Greene et al., 2019; Mahamkali et al., 2020), which are important for accounting for the effects from high extracellular product levels (e.g. acetate, ethanol).

Global Transcriptome Trends With Faster Growth

Next, we performed transcriptome analysis using RNA sequencing (RNA-seq) to quantify μ -dependent gene expression changes on both gas mixes. High reproducibility of the data was demonstrated by clear clustering of bio-replicates (**Figures 4A,B**) and an average Pearson correlation coefficient of $R = 0.96$ between bio-replicates across μ values (**Figure 4C**). Also,

significant μ -dependent expression differences for many genes could be seen for both gases (**Figure 4B**). Indeed, we determined 1,337 differentially expressed genes (DEGs) in total with a fold-change (FC) > 1.5 (up- or down-regulation) and a q -value < 0.05 after FDR correction in at least one pairwise comparison within the three pairwise μ -dependent comparisons ($\mu = 2.0$ vs. 1.0, 2.8 vs. 1.0, and 2.8 vs. 2.0 day^{-1}) of both gas mixes (**Supplementary Tables S4, S5**). Expectedly, the bigger the difference between compared μ values, the higher the number of DEGs (**Figure 4D**). Also, many DEGs were shared between comparisons within both gas mixes. Interestingly, while 442 DEGs were shared between CO and syngas comparisons of $\mu = 2.8$ vs. 1.0 day^{-1} , hundreds of unique DEGs were also detected, demonstrating the effect of the feed gas mix on μ -dependent gene expression patterns.

To understand global transcriptome changes that facilitate faster growth, we assessed DEGs through functional gene classifications. Firstly, analysis of DEGs of $\mu = 2.8$ vs. 1.0 day^{-1} using Cluster of Orthologous Groups (COG) classification (Tatusov et al., 2003) showed that most DEGs were classified as “Function unknown” (S) (**Figure 5A; Supplementary Table S6**). This highlights the need for genotype-phenotype mapping and improving gene

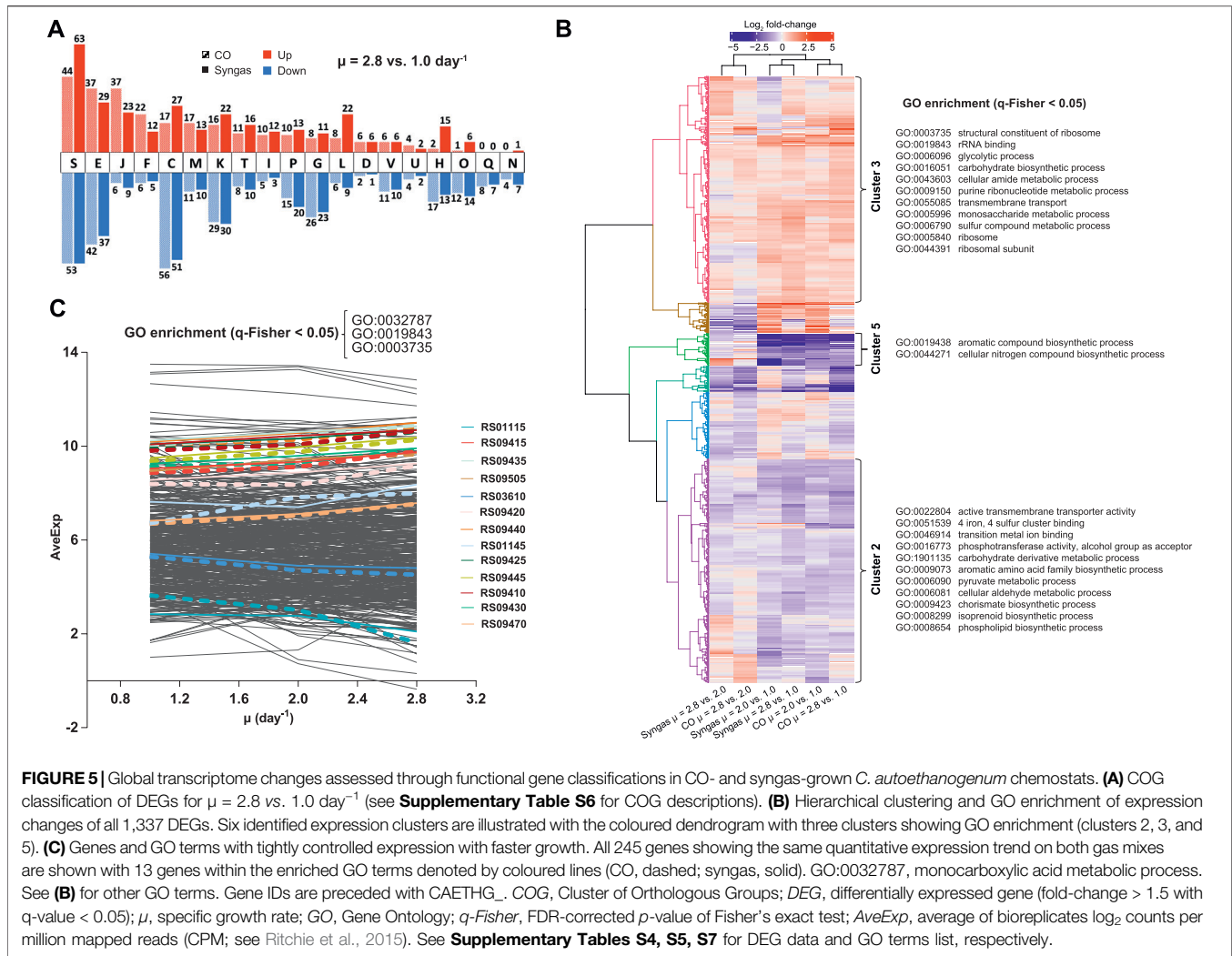


annotations for acetogens. Genes involved in energy, amino acid, and nucleotide metabolism (C, E, and F) and replication, transcription, and translation (J, K, and L) were also abundant among DEGs and all these processes are vital for faster growth. Secondly, we used Gene Ontology (GO) terms (Ashburner et al., 2000) to attain finer resolution behind global gene expression trends. Clustering of all 1,337 DEGs across μ comparisons and gas mixes resulted in six significant expression clusters (**Figure 5B**). GO enrichment analysis (q-Fisher < 0.05) of the genes within the identified clusters was consistent with COG analysis as several GO terms related to translation (0003735, 0019843, 0005840, and 0044391) and metabolism (0006096, 0016051, 0043603, 0009150, 00505996, and 0006790) were enriched in cluster 3 that includes up-regulated genes with faster growth. Enrichment of GO terms within clusters 2 and 5 was detected, including genes down-regulated with faster growth. Lastly, we aimed to identify genes and GO terms whose expression was tightly controlled with changing μ , indicated by the same expression trend on both gas mixes. We identified 245 such genes that showed either continuously increasing or decreasing differential expression (DEGs, i.e., FC > 1.5 and q < 0.05) with increasing μ on both gases with the same magnitude of expression change between the two gas mixes (**Figure 5C**). Enrichment analysis of these genes confirmed the aforementioned results by identifying

enrichment of genes (q-Fisher < 0.05) associated with translation (0003735 and 0019843), but also of the GO term 0032787 “monocarboxylic acid metabolic process” (coloured lines on **Figure 5C**).

Transcriptional Changes Linked to Metabolic Rearrangements

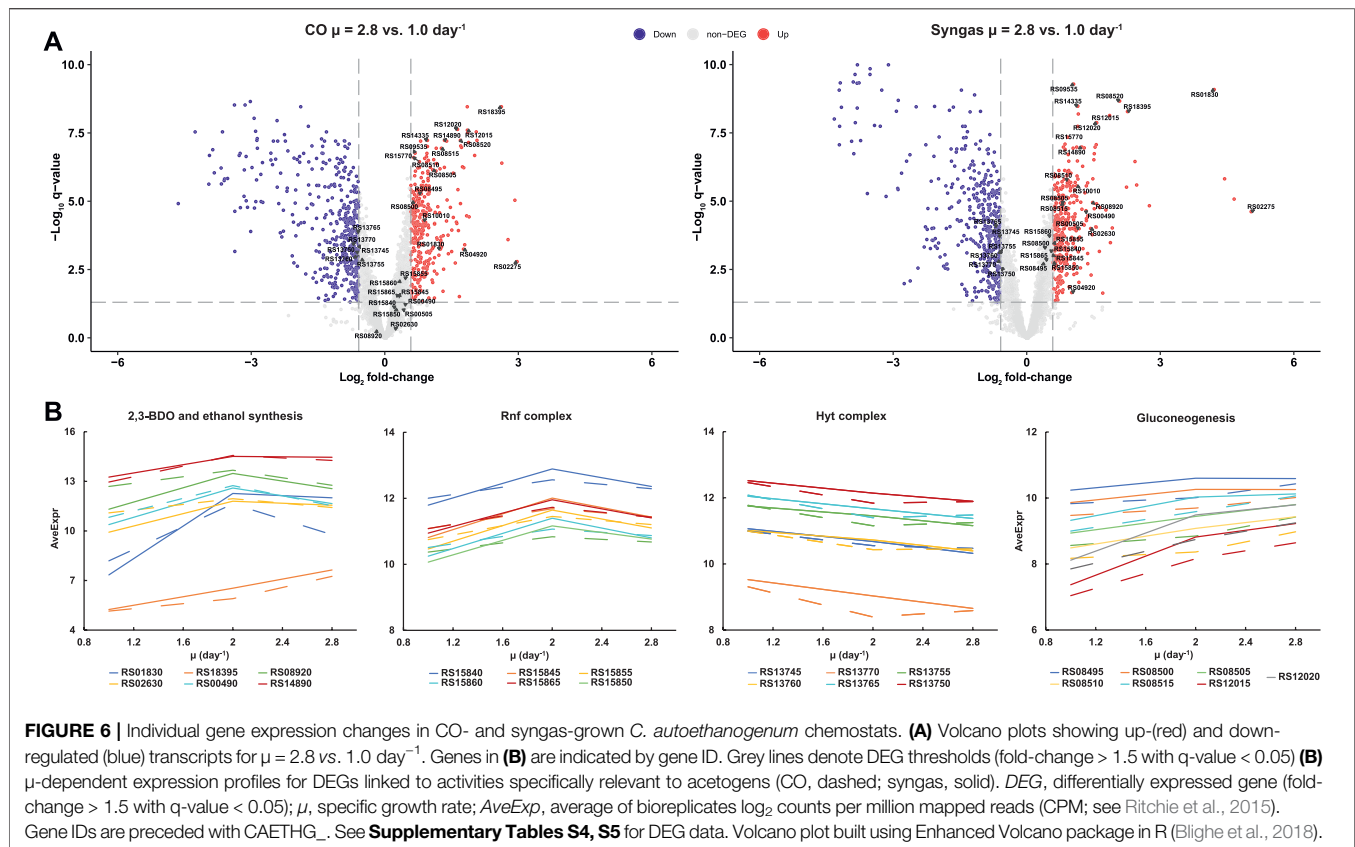
Previous transcriptomics and proteomics studies have suggested that autotrophic metabolism of acetogens is not controlled through hierarchical regulation of gene expression (Richter et al., 2016; Valgepea et al., 2017a, 2018; Al-bassam et al., 2018; Mahamkali et al., 2020). We thus analysed DEGs in terms of individual genes linked to activities specifically relevant to acetogens or with high expression changes. Surprisingly, we found numerous DEGs in central metabolism, some of which can explain the metabolic rearrangements described above (**Figure 6**; **Supplementary Figures S1, S2**). For instance, increased carbon flux to 2,3-BDO with faster growth on syngas (**Figure 2**) was supported by 18.5-fold (q < 0.01) (all $\mu = 2.8$ vs. 1.0 day⁻¹ unless otherwise noted) up-regulation of the 2,3-BDO dehydrogenase (CAETHG_RS01830; BDH) that reduces acetoin to 2,3-BDO and by 2.3-fold (q < 0.01) up-regulation of the pyruvate:Fd (flavodoxin) oxidoreductase (RS14890; PFOR) that converts



acetyl-CoA to pyruvate (**Figure 6**). At the same time, elevated production of ethanol (**Figure 2**) could be linked to increased expression (2.1- to 2.8-fold, $q < 0.01$) of several alcohol dehydrogenases (RS02620 and RS02630; Adh and Adh3), including the most abundant—RS08920; Adh4—in *C. autoethanogenum* (**Supplementary Table S4**) (Valgepea et al., 2017a, 2021) on syngas (**Figure 6**). Acetaldehyde for the alcohol dehydrogenases was likely not supplied directly from acetyl-CoA as we quantified strong repression of two putative acetaldehyde dehydrogenases (RS08810 and RS08865; 11.5- and 17.0-fold, $q < 0.01$), which interestingly seem to be the result of the uniformly strong repression of a cluster of 21 genes (RS08795–08895) linked to bacterial microcompartments (BMCs) (**Supplementary Figure S1**). Despite the 4.8-fold ($q < 0.01$) upregulation of one of the bifunctional aldehyde/alcohol dehydrogenases (RS18395; AdhE1) which catalyses ethanol production directly from acetyl-CoA, ethanol was still most likely produced through acetate using the AOR activity as AOR1 transcripts were ~160-fold more abundant (RPKM) compared to AdhE1 (**Supplementary Tables S2, S3**) across all experiments and AOR2 (RS00490)

was up-regulated 2.5-fold ($q < 0.01$) (**Supplementary Tables S4, S5**). This is consistent with metabolic flux data (**Figure 3**) and previous-omics and knockout experiments in acetogens (see above).

Faster growth demands more energy and this was supported by increased expression (1.5- to 2.2-fold, $q < 0.01$) of genes of the multi-subunit Fd-NAD⁺ oxidoreductase Rnf complex (RS15845–65) across the studied range of μ (**Figure 6**), as the Rnf complex generates the proton motive force to drive the ATPase in *C. autoethanogenum* (Hess et al., 2016; Tremblay et al., 2012). Notably, up-regulation of NAD(P)- (RS02275) and FAD-dependent (RS04920) oxidoreductases was also detected (7.9- to 32.9-fold and 2.0- to 3.4-fold, respectively, $q < 0.01$) on both gases that might play a role in the maintenance of redox homeostasis (**Supplementary Figure S2**). Intriguingly, despite the elevated H₂ uptake with faster growth on syngas (**Figure 1C**), ~1.5-fold ($q < 0.01$) repression of the main H₂ oxidiser—the HytA-E complex (RS13745–70)—(Wang et al., 2013; Mock et al., 2015; Valgepea et al., 2021) components was seen (**Figure 6**). Moreover, similar down-regulation was observed in CO cultures, potentially



indicating μ -dependent regulation of the HytA-E complex. Repression of HytA-E also means that gene expression levels at $\mu = 1.0 \text{ day}^{-1}$ were sufficient to realise higher H₂ uptake with faster growth, which was also the case for higher CO fixation as WLP genes were not detected as DEGs (**Supplementary Tables S4, S5**). In contrast, increased flux throughput for biomass synthesis with faster growth was supported by elevated expression of gluconeogenesis genes (RS08495–08515, RS12015, and RS12020) (**Figure 6B**). In the future, further work using genetically modified strains is needed to determine whether any of the putative transcription factors that were up-regulated with faster growth (**Supplementary Figure S2**) are responsible for increased gene expression in any of the cases above.

DISCUSSION

Exploring the physiological boundaries of acetogens has been informative for understanding regulation of their energy-limited metabolism (Valgepea et al., 2017a; Klask et al., 2020; Mahamkali et al., 2020; Jin et al., 2021). Additionally, various bioprocess approaches, multi-omics analysis, construction of metabolic models, and development of genetic tools are being pursued for development of cell factories with enhanced substrate conversion, product distribution, and expanded product spectrum (Valgepea et al., 2018; Lemgruber et al., 2019;

Molitor et al., 2019; Heffernan et al., 2020; Smith et al., 2020; Bourgade et al., 2021; Diender et al., 2021; Fackler et al., 2021; Jin et al., 2021; Pavan et al., 2022). Notably, the effects of μ on acetogen metabolism and the gas fermentation bioprocess have not been established. Here, we investigated the μ -dependent bioprocess performance of the acetogen *C. autoethanogenum* in CO- and syngas-grown steady-state chemostat cultures and assessed metabolic responses using gas analysis, metabolomics, transcriptomics, and metabolic modelling.

We observed higher carbon flux towards ethanol and 2,3-BDO production with faster growth on syngas (**Figure 2**). Increased carbon flux to the same reduced products is also seen with higher steady-state biomass concentrations for syngas-fermenting *C. autoethanogenum* cultures (Valgepea et al., 2017a). Furthermore, we also measured significantly increased specific productivities of ethanol (q_{EtOH}) and 2,3-BDO ($q_{2,3\text{-BDO}}$) with faster growth (**Figure 1B**). These trends are beneficial for an industrial gas fermentation process as faster growth and higher biomass levels complimentary lead to higher product yields and volumetric productivities (g/L/h). The fact that no clear trend between μ and carbon flux to 2,3-BDO was seen for CO-grown cultures (**Figure 2**) confirms that feed gas composition has a substantial effect on acetogen product distribution (Diender et al., 2016; Xu et al., 2017; Valgepea et al., 2018; Jack et al., 2019; Heffernan et al., 2020). While cells used the majority of the H₂ supplied within syngas to directly reduce CO₂ to formate in the WLP (**Figure 3**), H₂ supply also had a direct effect on intracellular

redox homeostasis as H_2 oxidation provided up to 10% of the total Fd_{red} generated by the cells (**Supplementary Table S8**), which is consistent with previous observations in *C. autoethanogenum* (Valgepea et al., 2017a, 2018).

Our transcriptomics data revealed differential expression for more than a thousand genes (DEGs) with increasing μ (**Supplementary Tables S4, S5**). This means that the acetogen *C. autoethanogenum* uses transcriptional regulation to a large extent at least for facilitating faster growth, compared to previous omics studies that suggest a limited role for hierarchical regulation of gene expression in autotrophic metabolism (Richter et al., 2016; Valgepea et al., 2017a, 2018; Al-bassam et al., 2018; Mahamkali et al., 2020). In addition to DEGs linked to activities specifically relevant to acetogens (e.g., oxidoreductases, hydrogenases, alcohol/aldehyde dehydrogenases), the functional classification analysis identified genes related to translation within DEGs up-regulated with faster growth (**Figure 5**). This indicates that the well-known positive correlation between μ and total RNA content of biomass (Schaechter et al., 1958) is not sufficient for ensuring faster growth of acetogens either, similarly to μ -dependent datasets for other microbes (Regenberg et al., 2006; Ishii et al., 2007; Valgepea et al., 2010; Lahtvee et al., 2011). Notably, COG classification of DEGs identified most genes within the group “Function unknown” (S) (**Figure 5A**), while DEGs also included many genes with unclear functions for autotrophic growth, e.g., sugar, amino acid, and other transporters, hypothetical proteins, BMC-related genes (**Supplementary Tables S4, S5**). This highlights the need for mapping genotype-phenotype links and improving gene annotations for advancing understanding of acetogen metabolism and engineering of cell factories.

Though our chemostat cultures were CO-limited and thus the residual CO concentration in the liquid phase was low, elevated CO feeding could still inhibit cellular hydrogenases and hence H_2 uptake for syngas cultures (Thauer et al., 1974; Wang et al., 2013; Mahamkali et al., 2020). Higher syngas, and thus also CO, feeding rates to support faster growth did not, however, prevent elevated H_2 uptake (**Figure 1C**). Interestingly, expression of genes responsible for realising higher H_2 uptake—HytA-E for H_2 oxidation and its complex partner FdhA for direct CO_2 reduction to formate using H_2 —was not increased at the same time (**Figure 6**). This is consistent with proteomics data showing no expression change of hydrogenase proteins even when *C. autoethanogenum* increases its H_2 uptake from near-zero to ~ 30 mmol/gDCW/h (Valgepea et al., 2018). Similarly, we could neither detect up-regulation of any WLP genes with substantially increased flux through the pathway with faster growth. However, the expression of gluconeogenesis genes was increased to support faster biomass synthesis (**Figure 6**). These observations suggest evolutionary prioritisation of pathways in *C. autoethanogenum* to ensure sufficient “baseline” enzymatic capacity for increasing flux throughput through key catabolic pathways for CO and H_2 metabolism, consistent with integrative analysis in *C. autoethanogenum* (Valgepea et al., 2021) and other microbes (Daran-Lapujade et al., 2007; Adamberg et al., 2012;

Valgepea et al., 2013). This would also provide acetogens an advantage in their natural environments as cells could rapidly respond to CO and H_2 availability without delays to kick-start metabolism.

Our transcriptomics data are also informative regarding by-product synthesis. In a closely related acetogen—*C. ljungdahlii*—gene expression of all 2,3-BDO production pathway genes is increased prior to 2,3-BDO production in autotrophic batch cultures (Köpke et al., 2011). We, however, detected strong up-regulation (18.5-fold) of only BDH (RS01830; reduces acetoin to 2,3-BDO) with substantially increased carbon flux to 2,3-BDO with faster growth on syngas despite the 2,3-BDO production pathway genes being nearly identical between the two species (Brown et al., 2014). This potentially suggests that there is no transcriptional limitation for channelling carbon from pyruvate to acetoin and makes BDH a protein and metabolic engineering target for improving 2,3-BDO production in *C. autoethanogenum*. While our transcriptomics and metabolic modelling results confirmed the dominant role of AOR activities for ethanol biosynthesis in acetogens (Marcellin et al., 2016; Valgepea et al., 2018; Heffernan et al., 2020; Liew et al., 2017; Richter et al., 2016), strong repression of a cluster of 21 genes (RS08795–08895) linked to BMCs including two putative acetaldehyde dehydrogenases (RS08810 and RS08865) was detected (**Supplementary Figure S1**). Clustering of putative alcohol and acetaldehyde dehydrogenases within BMC-encoding genes in *C. autoethanogenum* has been noted before (Mock et al., 2015). Cells use BMCs to optimise metabolic pathways by encapsulating enzymes within a protein shell to trap toxic intermediates (Chowdhury et al., 2014; Kerfeld and Erbilgin, 2015). While BMCs seem to play an important role for heterotrophic growth of the acetogen *Acetobacterium woodii* (Schuchmann et al., 2015; Chowdhury et al., 2020; Chowdhury et al., 2021), it remains to be seen how relevant are BMCs for *C. autoethanogenum* autotrophy as the 21 gene cluster was expressed at very low abundances (**Supplementary Tables S2, S3**).

Overall, our study provides important quantitative information and systems-level analysis of the effects of the key physiological parameter— μ —on acetogen metabolism and the gas fermentation bioprocess during steady-state cultures. We conclude that the bioprocess benefits from faster growth of *C. autoethanogenum* by supporting both higher product yields and productivities. Furthermore, our work advances understanding of transcriptional regulation in acetogens and supports the concept that cells maintain sufficient “baseline” expression of key catabolic pathways for increasing flux throughput. Finally, differential expression of genes with unclear functions emphasises the need for mapping genotype-phenotype links and improving gene annotations for advancing understanding of acetogen metabolism and engineering of cell factories.

DATA AVAILABILITY STATEMENT

RNA sequencing data have been deposited in the NCBI Gene Expression Omnibus repository under accession number GSE196640.

AUTHOR CONTRIBUTIONS

LADL: Conceptualization, Methodology, Formal analysis, Investigation, Writing–Original Draft, Writing–Review and Editing; HI: Methodology, Formal analysis, Investigation, Writing–Review and Editing; KB: Investigation; KR: Methodology, Formal analysis, Writing–Review and Editing; CB: Software, Resources, Writing–Review and Editing; AH: Resources, Writing–Review and Editing, Project Administration; EM: Resources, Writing–Review and Editing; MK: Conceptualisation, Resources, Writing–Review and Editing; KV: Conceptualization, Methodology, Formal analysis, Investigation, Resources, Writing–Original Draft, Writing–Review and Editing; Supervision, Project Administration, Funding Acquisition.

FUNDING

This work was funded by the European Union’s Horizon 2020 research and innovation programme under grant agreement N810755 and the Estonian Research Council’s grant

REFERENCES

- Abubackar, H. N., Veiga, M. C., and Kennes, C. (2012). Biological Conversion of Carbon Monoxide to Ethanol: Effect of pH, Gas Pressure, Reducing Agent and Yeast Extract. *Bioresour. Technology* 114, 518–522. doi:10.1016/j.biortech.2012.03.027
- Abubackar, H. N., Veiga, M. C., and Kennes, C. (2015). Carbon Monoxide Fermentation to Ethanol by *Clostridium autoethanogenum* in a Bioreactor with No Accumulation of Acetic Acid. *Bioresour. Technology* 186, 122–127. doi:10.1016/j.biortech.2015.02.113
- Adamberg, K., Seiman, A., and Vilu, R. (2012). Increased Biomass Yield of *Lactococcus lactis* by Reduced Overconsumption of Amino Acids and Increased Catalytic Activities of Enzymes. *PLoS One* 7, e48223. doi:10.1371/journal.pone.0048223
- Adamberg, K., Valgepea, K., and Vilu, R. (2015). Advanced Continuous Cultivation Methods for Systems Microbiology. *Microbiology* 161 (9), 1707–1719. doi:10.1099/mic.0.000146
- Al-bassam, M. M., Kim, J.-N., Zaramela, L. S., Kellman, B. P., Zuniga, C., Wozniak, J. M., et al. (2018). Optimization of Carbon and Energy Utilization through Differential Translational Efficiency. *Nat. Commun.* 9, 4474. doi:10.1038/s41467-018-06993-6
- Alexa, A., and Rahnenfuhrer, J. (2020). *topGO: Enrichment Analysis for Gene Ontology*. R package version 2.42.0.
- Ashburner, M., Ball, C. A., Blake, J. A., Botstein, D., Butler, H., Cherry, J. M., et al. (2000). Gene Ontology: Tool for the Unification of Biology. *Nat. Genet.* 25, 25–29. doi:10.1038/75556
- Benjamini, Y., and Hochberg, Y. (1995). Controlling the False Discovery Rate: a Practical and Powerful Approach to Multiple Testing. *J. R. Stat. Soc. Ser. B (Methodological)* 57 (1), 289–300. doi:10.1111/j.2517-6161.1995.tb02031.x
- Blighe, K., Rana, S., and Lewis, M. (2018). EnhancedVolcano: Publication-Ready Volcano Plots with Enhanced Colouring and Labeling. Available at: <https://github.com/kevinblighe/EnhancedVolcano> (Accessed March 15, 2021).
- Bourgade, B., Minton, N. P., and Islam, M. A. (2021). Genetic and Metabolic Engineering Challenges of C1-Gas Fermenting Acetogenic Chassis Organisms. *FEMS Microbiol. Rev. Fuab008* 45, 1–20. doi:10.1093/femsre/fuab008
- Brown, S. D., Nagaraju, S., Utturkar, S., De Tissera, S., Segovia, S., Mitchell, W., et al. (2014). Comparison of Single-Molecule Sequencing and Hybrid Approaches for Finishing the Genome of *Clostridium autoethanogenum* and

agreement PSG289. Australian Government funding through its investment agency, the Australian Research Council, towards the ARC Centre of Excellence in Synthetic Biology (CE200100029) is gratefully acknowledged.

ACKNOWLEDGMENTS

We thank the following investors in LanzaTech’s technology: BASF, CICC Growth Capital Fund I, CITIC Capital, Indian Oil Company, K1W1, Khosla Ventures, the Malaysian Life Sciences, Capital Fund, L. P., Mitsui, the New Zealand Superannuation Fund, Novo Holdings A/S, Petronas Technology Ventures, Primetals, Qiming Venture Partners, Softbank China, and Suncor.

SUPPLEMENTARY MATERIAL

The Supplementary Material for this article can be found online at: <https://www.frontiersin.org/articles/10.3389/fbioe.2022.879578/full#supplementary-material>

- Analysis of CRISPR Systems in Industrial Relevant Clostridia. *Biotechnol. Biofuels* 7, 40. doi:10.1186/1754-6834-7-40
- Chowdhury, C., Sinha, S., Chun, S., Yeates, T. O., and Bobik, T. A. (2014). Diverse Bacterial Microcompartment Organelles. *Microbiol. Mol. Biol. Rev.* 78 (3), 438–468. doi:10.1128/mmb.00009-14
- Chowdhury, N. P., Alberti, L., Linder, M., and Müller, V. (2020). Exploring Bacterial Microcompartments in the Acetogenic Bacterium *Acetobacterium woodii*. *Front. Microbiol.* 11, 593467. doi:10.3389/fmicb.2020.593467
- Chowdhury, N. P., Moon, J., and Müller, V. (2021). Adh4, an Alcohol Dehydrogenase Controls Alcohol Formation within Bacterial Microcompartments in the Acetogenic Bacterium *Acetobacterium woodii*. *Environ. Microbiol.* 23 (1), 499–511. doi:10.1111/1462-2920.15340
- Cotter, J. L., Chinn, M. S., and Grunden, A. M. (2009). Influence of Process Parameters on Growth of *Clostridium Ljungdahlii* and *Clostridium autoethanogenum* on Synthesis Gas. *Enzyme Microb. Technology* 44 (5), 281–288. doi:10.1016/j.enzmictec.2008.11.002
- Cotton, C. A., Edlich-Muth, C., and Bar-Even, A. (2018). Reinforcing Carbon Fixation: CO₂ Reduction Replacing and Supporting Carboxylation. *Curr. Opin. Biotechnol.* 49, 49–56. doi:10.1016/j.copbio.2017.07.014
- Daran-Lapujade, P., Rossell, S., van Gulik, W. M., Luttkik, M. A. H., de Groot, M. J. L., Slijper, M., et al. (2007). The Fluxes through Glycolytic Enzymes in *Saccharomyces cerevisiae* Are Predominantly Regulated at Posttranscriptional Levels. *Proc. Natl. Acad. Sci. U.S.A.* 104, 15753–15758. doi:10.1073/pnas.0707476104
- de Souza Pinto Lemgruber, R., Valgepea, K., Gonzalez Garcia, R. A., de Bakker, C., Palfreyman, R. W., Tappel, R., et al. (2019). A TetR-Family Protein (CAETHG_0459) Activates Transcription from a New Promoter Motif Associated with Essential Genes for Autotrophic Growth in Acetogens. *Front. Microbiol.* 10, 2549. doi:10.3389/fmicb.2019.02549
- Diender, M., Parera Olm, I., Gelderloos, M., Koehorst, J. J., Schaap, P. J., Stams, A. J. M., et al. (2019). Metabolic Shift Induced by Synthetic Co-cultivation Promotes High Yield of Chain Elongated Acids from Syngas. *Sci. Rep.* 9 (1), 18081. doi:10.1038/s41598-019-54445-y
- Diender, M., Parera Olm, I., and Sousa, D. Z. (2021). Synthetic Co-cultures: Novel Avenues for Bio-Based Processes. *Curr. Opin. Biotechnol.* 67, 72–79. doi:10.1016/j.copbio.2021.01.006
- Diender, M., Stams, A. J. M., and Sousa, D. Z. (2016). Production of Medium-Chain Fatty Acids and Higher Alcohols by a Synthetic Co-culture Grown on Carbon Monoxide or Syngas. *Biotechnol. Biofuels* 9 (1), 82. doi:10.1186/s13068-016-0495-0

- Drake, H. L., Küsel, K., and Matthies, C. (2006). Acetogenic Prokaryotes. *Prokaryotes* 2, 354–420. doi:10.1007/0-387-30742-7_13
- Esquivel-Elizondo, S., Delgado, A. G., Rittmann, B. E., and Krajmalnik-Brown, R. (2017). The Effects of CO₂ and H₂ on CO Metabolism by Pure and Mixed Microbial Cultures. *Biotechnol. Biofuels*. 10 (1), 220. doi:10.1186/s13068-017-0910-1
- Ewels, P., Magnusson, M., Lundin, S., and Käller, M. (2016). MultiQC: Summarize Analysis Results for Multiple Tools and Samples in a Single Report. *Bioinformatics* 32 (19), 3047–3048. doi:10.1093/bioinformatics/btw354
- Fackler, N., Heijstra, B. D., Rasor, B. J., Brown, H., Martin, J., Ni, Z., et al. (2021). Stepping on the Gas to a Circular Economy: Accelerating Development of Carbon-Negative Chemical Production from Gas Fermentation. *Annu. Rev. Chem. Biomol. Eng.* 12 (1), 439–470. doi:10.1146/annurev-chembioeng-120120-021122
- Fast, A. G., and Papoutsakis, E. T. (2012). Stoichiometric and Energetic Analyses of Non-photosynthetic CO₂-fixation Pathways to Support Synthetic Biology Strategies for Production of Fuels and Chemicals. *Curr. Opin. Chem. Eng.* 1 (4), 380–395. doi:10.1016/j.coche.2012.07.005
- Galili, T. (2015). Dendextend: An R Package for Visualizing, Adjusting and Comparing Trees of Hierarchical Clustering. *Bioinformatics* 31 (22), 3718–3720. doi:10.1093/bioinformatics/btv428
- Greene, J., Daniell, J., Köpke, M., Broadbelt, L., and Tyo, K. E. J. (2019). Kinetic Ensemble Model of Gas Fermenting *Clostridium autoethanogenum* for Improved Ethanol Production. *Biochem. Eng. J.* 148, 46–56. doi:10.1016/j.bej.2019.04.021
- Gu, Z., Eils, R., and Schlesner, M. (2016). Complex Heatmaps Reveal Patterns and Correlations in Multidimensional Genomic Data. *Bioinformatics* 32 (18), 2847–2849. doi:10.1093/bioinformatics/btw313
- Hackett, S. R., Zanotelli, V. R. T., Xu, W., Goya, J., Park, J. O., Perlman, D. H., et al. (2016). Systems-level Analysis of Mechanisms Regulating Yeast Metabolic Flux. *Science* 354, aaf2786. doi:10.1126/science.aaf2786
- Heffernan, J. K., Valgepea, K., de Souza Pinto Lemgruber, R., Casini, I., Plan, M., Tappel, R., et al. (2020). Enhancing CO₂-Valorization Using *Clostridium autoethanogenum* for Sustainable Fuel and Chemicals Production. *Front. Bioeng. Biotechnol.* 8, 204. doi:10.3389/fbioe.2020.00204
- Hess, V., Gallegos, R., Jones, J. A., Barquera, B., Malamy, M. H., and Müller, V. (2016). Occurrence of ferredoxin:NAD+oxidoreductase Activity and its Ion Specificity in Several Gram-Positive and Gram-Negative Bacteria. *PeerJ* 4, e1515. doi:10.7717/peerj.1515
- Huerta-Cepas, J., Szklarczyk, D., Heller, D., Hernández-Plaza, A., Forslund, S. K., Cook, H., et al. (2019). eggNOG 5.0: a Hierarchical, Functionally and Phylogenetically Annotated Orthology Resource Based on 5090 Organisms and 2502 Viruses. *Nucleic Acids Res.* 47, D309–D314. doi:10.1093/nar/gky1085
- Ishii, N., Nakahigashi, K., Baba, T., Robert, M., Soga, T., Kanai, A., et al. (2007). Multiple High-Throughput Analyses Monitor the Response of *E. coli* to Perturbations. *Science* 316, 593–597. doi:10.1126/science.1132067
- Jack, J., Lo, J., Maness, P.-C., and Ren, Z. J. (2019). Directing *Clostridium ljungdahlii* Fermentation Products via Hydrogen to Carbon Monoxide Ratio in Syngas. *Biomass and Bioenergy* 124, 95–101. doi:10.1016/j.biombioe.2019.03.011
- Jin, S., Jeon, Y., Jeon, M. S., Shin, J., Song, Y., Kang, S., et al. (2021). Acetogenic Bacteria Utilize Light-Driven Electrons as an Energy Source for Autotrophic Growth. *Proc. Natl. Acad. Sci. U.S.A.* 118 (9), e2020552118. doi:10.1073/pnas.2020552118
- Jones, P., Binns, D., Chang, H.-Y., Fraser, M., Li, W., McAnulla, C., et al. (2014). InterProScan 5: Genome-Scale Protein Function Classification. *Bioinformatics* 30 (9), 1236–1240. doi:10.1093/bioinformatics/btu031
- Kerfeld, C. A., and Erbilgin, O. (2015). Bacterial Microcompartments and the Modular Construction of Microbial Metabolism. *Trends Microbiol.* 23 (1), 22–34. doi:10.1016/j.tim.2014.10.003
- Klask, C.-M., Kliem-Kuster, N., Molitor, B., and Angenent, L. T. (2020). Nitrate Feed Improves Growth and Ethanol Production of *Clostridium ljungdahlii* with CO₂ and H₂, but Results in Stochastic Inhibition Events. *Front. Microbiol.* 11, 724. doi:10.3389/fmicb.2020.00724
- Köpke, M., Mihalcea, C., Liew, F., Tizard, J. H., Ali, M. S., Conolly, J. J., et al. (2011). 2,3-Butanediol Production by Acetogenic Bacteria, an Alternative Route to Chemical Synthesis, Using Industrial Waste Gas. *Appl. Environ. Microbiol.* 77 (15), 5467–5475. doi:10.1128/AEM.00355-11
- Köpke, M., and Simpson, S. D. (2020). Pollution to Products: Recycling of 'above Ground' Carbon by Gas Fermentation. *Curr. Opin. Biotechnol.* 65, 180–189. doi:10.1016/j.copbio.2020.02.017
- Lahtvee, P.-J., Adamberg, K., Arike, L., Nahku, R., Aller, K., and Vilu, R. (2011). Multi-omics Approach to Study the Growth Efficiency and Amino Acid Metabolism in *Lactococcus Lactis* at Various Specific Growth Rates. *Microb. Cel. Fact.* 10, 1–12. doi:10.1186/1475-2859-10-12
- Li, H., Handsaker, B., Wysoker, A., Fennell, T., Ruan, J., Homer, N., et al. (2009). The Sequence Alignment/Map Format and SAMtools. *Bioinformatics* 25 (16), 2078–2079. doi:10.1093/bioinformatics/btp352
- Liao, Y., Smyth, G. K., and Shi, W. (2019). The R Package Rsubread Is Easier, Faster, Cheaper and Better for Alignment and Quantification of RNA Sequencing Reads. *Nucleic Acids Res.* 47, e47. doi:10.1093/nar/gkz114
- Liew, F., Henstra, A. M., Köpke, M., Winzer, K., Simpson, S. D., and Minton, N. P. (2017). Metabolic Engineering of *Clostridium autoethanogenum* for Selective Alcohol Production. *Metab. Eng.* 40, 104–114. doi:10.1016/j.ymben.2017.01.007
- Liew, F., Martin, M. E., Tappel, R. C., Heijstra, B. D., Mihalcea, C., and Köpke, M. (2016). Gas Fermentation-A Flexible Platform for Commercial Scale Production of Low-Carbon-Fuels and Chemicals from Waste and Renewable Feedstocks. *Front. Microbiol.* 7, 694. doi:10.3389/fmicb.2016.00694
- Lipson, D. A. (2015). The Complex Relationship between Microbial Growth Rate and Yield and its Implications for Ecosystem Processes. *Front. Microbiol.* 6 (JUN), 1–5. doi:10.3389/fmicb.2015.00615
- Mahamkali, V., Valgepea, K., de Souza Pinto Lemgruber, R., Plan, M., Tappel, R., Köpke, M., et al. (2020). Redox Controls Metabolic Robustness in the Gas-Fermenting Acetogen *Clostridium autoethanogenum*. *Proc. Natl. Acad. Sci. U.S.A.* 117, 13168–13175. doi:10.1073/pnas.1919531117
- Marcellin, E., Behrendorf, J. B., Nagaraju, S., DeTissera, S., Segovia, S., Palfreyman, R. W., et al. (2016). Low Carbon Fuels and Commodity Chemicals from Waste Gases - Systematic Approach to Understand Energy Metabolism in a Model Acetogen. *Green. Chem.* 18, 3020–3028. doi:10.1039/C5GC02708J
- Martin, M. (2011). Cutadapt Removes Adapter Sequences from High-Throughput Sequencing Reads. *EMBnet j.* 17 (1), 10–12. doi:10.14806/ej.17.1.200
- Martin, M. E., Richter, H., Saha, S., and Angenent, L. T. (2015). Traits of selected *Clostridium* strains for Syngas Fermentation to Ethanol. *Biotechnol. Bioeng.* 113 (3), 531–539. doi:10.1002/bit.25827
- Mock, J., Zheng, Y., Mueller, A. P., Ly, S., Tran, L., Segovia, S., et al. (2015). Energy Conservation Associated with Ethanol Formation from H₂ and CO₂ in *Clostridium autoethanogenum* Involving Electron Bifurcation. *J. Bacteriol.* 197 (18), 2965–2980. doi:10.1128/JB.00399-15
- Molitor, B., Marcellin, E., and Angenent, L. T. (2017). Overcoming the Energetic Limitations of Syngas Fermentation. *Curr. Opin. Chem. Biol.* 41, 84–92. doi:10.1016/j.cbpa.2017.10.003
- Molitor, B., Mishra, A., and Angenent, L. T. (2019). Power-to-protein: Converting Renewable Electric Power and Carbon Dioxide into Single Cell Protein with a Two-Stage Bioprocess. *Energy Environ. Sci.* 12, 3515–3521. doi:10.1039/c9ee02381j
- Molitor, B., Richter, H., Martin, M. E., Jensen, R. O., Juminaga, A., Mihalcea, C., et al. (2016). Carbon Recovery by Fermentation of CO-rich off Gases - Turning Steel Mills into Biorefineries. *Bioresour. Technology* 215, 386–396. doi:10.1016/j.biortech.2016.03.094
- O'Brien, E. J., Monk, J. M., and Palsson, B. O. (2015). Using Genome-Scale Models To Predict Biological Capabilities. *Cell* 161 (5), 971–987. doi:10.1016/j.cell.2015.05.019
- Orth, J. D., Thiele, I., and Palsson, B. O. (2010). What is Flux Balance Analysis?. *Nat. Biotechnol.* 28 (3), 245–248. doi:10.1038/nbt.1614
- Park, S., Ahn, B., and Kim, Y.-K. (2019). Growth Enhancement of Bioethanol-Producing Microbe *Clostridium Autoethanogenum* by Changing Culture Medium Composition. *Bioresour. Technology Rep.* 6, 237–240. doi:10.1016/j.biteb.2019.03.012
- Pavan, M., Reimmets, K., Garg, S., Mueller, A. P., Marcellin, E., Köpke, M., et al. (2022). Advances in Systems Metabolic Engineering of Autotrophic Carbon

- Oxide-Fixing Biocatalysts towards a Circular Economy. *Metab. Eng.* 1, 1. doi:10.1016/j.ymben.2022.01.015
- Peebo, K., Valgepea, K., Maser, A., Nahku, R., Adamberg, K., and Vilu, R. (2015). Proteome Reallocation in *Escherichia coli* with Increasing Specific Growth Rate. *Mol. Biosyst.* 11 (4), 1184–1193. doi:10.1039/c4mb00721b
- Peebo, K., Valgepea, K., Nahku, R., Riis, G., Öun, M., Adamberg, K., et al. (2014). Coordinated Activation of PTA-ACS and TCA Cycles Strongly Reduces Overflow Metabolism of Acetate in *Escherichia coli*. *Appl. Microbiol. Biotechnol.* 98 (11), 5131–5143. doi:10.1007/s00253-014-5613-y
- Ragsdale, S. W., and Pierce, E. (2008). Acetogenesis and the Wood-Ljungdahl Pathway of CO₂ Fixation. *Biochim. Biophys. Acta (Bba) - Proteins Proteomics* 1784 (12), 1873–1898. doi:10.1016/j.bbapap.2008.08.012
- Redl, S., Diender, M., Jensen, T. Ø., Sousa, D. Z., and Nielsen, A. T. (2017). Exploiting the Potential of Gas Fermentation. *Ind. Crops Prod.* 106, 21–30. doi:10.1016/j.indcrop.2016.11.015
- Regenberg, B., Grotkjær, T., Winther, O., Fausbøll, A., Åkesson, M., Bro, C., et al. (2006). Growth-rate Regulated Genes Have Profound Impact on Interpretation of Transcriptome Profiling in *Saccharomyces cerevisiae*. *Genome Biol.* 7 (11), R107. doi:10.1186/gb-2006-7-11-r107
- Richter, H., Martin, M., and Angenent, L. (2013). A Two-Stage Continuous Fermentation System for Conversion of Syngas into Ethanol. *Energies* 6 (8), 3987–4000. doi:10.3390/en6083987
- Richter, H., Molitor, B., Wei, H., Chen, W., Aristilde, L., and Angenent, L. T. (2016). Ethanol Production in Syngas-Fermenting *Clostridium ljungdahlii* Is Controlled by Thermodynamics rather Than by Enzyme Expression. *Energ. Environ. Sci.* 9 (7), 2392–2399. doi:10.1039/C6EE01108J
- Ritchie, M. E., Phipson, B., Wu, D., Hu, Y., Law, C. W., Shi, W., et al. (2015). Limma powers Differential Expression Analyses for RNA-Sequencing and Microarray Studies. *Nucleic Acids Res.* 43 (7), e47. doi:10.1093/nar/gkv007
- Robinson, M. D., McCarthy, D. J., and Smyth, G. K. (2010). edgeR: A Bioconductor Package for Differential Expression Analysis of Digital Gene Expression Data. *Bioinformatics* 26 (1), 139–140. doi:10.1093/bioinformatics/btp616
- Schaechter, M., MaalOe, O., and Kjeldgaard, N. O. (1958). Dependency on Medium and Temperature of Cell Size and Chemical Composition during Balanced Growth of *Salmonella typhimurium*. *J. Gen. Microbiol.* 19, 592–606. doi:10.1099/00221287-19-3-592
- Schellenberger, J., Que, R., Fleming, R. M. T., Thiele, I., Orth, J. D., Feist, A. M., et al. (2011). Quantitative Prediction of Cellular Metabolism with Constraint-Based Models: the COBRA Toolbox v2.0. *Nat. Protoc.* 6 (9), 1290–1307. doi:10.1038/nprot.2011.308
- Schuchmann, K., and Müller, V. (2014). Autotrophy at the Thermodynamic Limit of Life: a Model for Energy Conservation in Acetogenic Bacteria. *Nat. Rev. Microbiol.* 12 (12), 809–821. doi:10.1038/nrmicro3365
- Schuchmann, K., Schmidt, S., Martinez Lopez, A., Kaberline, C., Kuhns, M., Lorenzen, W., et al. (2015). Nonacetogenic Growth of the Acetogen *Acetobacterium Woodii* on 1,2-propanediol. *J. Bacteriol.* 197 (2), 382–391. doi:10.1128/JB.02383-14
- Shin, J., Song, Y., Kang, S., Jin, S., Lee, J.-K., Kim, D. R., et al. (2021). Genome-Scale Analysis of *Acetobacterium woodii* Identifies Translational Regulation of Acetogenesis. *mSystems* 6, e0069621. doi:10.1128/MSYSTEMS.00696-21
- Smith, N. W., Shorten, P. R., Altermann, E., Roy, N. C., and McNabb, W. C. (2020). Mathematical Modelling Supports the Existence of a Threshold Hydrogen Concentration and media-dependent Yields in the Growth of a Reductive Acetogen. *Bioproc. Biosyst. Eng.* 43, 885–894. doi:10.1007/s00449-020-02285-w
- Song, Y., Shin, J., Jeong, Y., Jin, S., Lee, J.-K., Kim, D. R., et al. (2017). Determination of the Genome and Primary Transcriptome of Syngas Fermenting *Eubacterium limosum* ATCC 8486. *Sci. Rep.* 7 (1), 13694. doi:10.1038/s41598-017-14123-3
- Song, Y., Shin, J., Jin, S., Lee, J.-K., Kim, D. R., Kim, S. C., et al. (2018). Genome-scale Analysis of Syngas Fermenting Acetogenic Bacteria Reveals the Translational Regulation for its Autotrophic Growth. *BMC Genomics* 19, 837. doi:10.1186/s12864-018-5238-0
- Tatusov, R. L., Fedorova, N. D., Jackson, J. D., Jacobs, A. R., Kiryutin, B., Koonin, E. V., et al. (2003). The COG Database: an Updated Version Includes Eukaryotes. *BMC Bioinformatics* 4, 41. doi:10.1186/1471-2105-4-41
- Thauer, R. K., Kafer, B., Jungermann, K., and Zahringer, M. (1974). The Reaction of the Iron-Sulfur Protein Hydrogenase with Carbon Monoxide. *Eur. J. Biochem.* 42 (2), 447–452. doi:10.1111/j.1432-1033.1974.tb03358.x
- Törönen, P., Medlar, A., and Holm, L. (2018). PANNZER2: A Rapid Functional Annotation Web Server. *Nucleic Acids Res.* 46 (W1), W84–W88. doi:10.1093/nar/gky350
- Tremblay, P.-L., Zhang, T., Dar, S. A., Leang, C., and Lovley, D. R. (2013). The Rnf Complex of *Clostridium ljungdahlii* is a Proton-Translocating Ferredoxin:NAD + Oxidoreductase Essential for Autotrophic Growth. *MBio* 4 (1), e00406–12. doi:10.1128/mBio.00406-12
- Valgepea, K., Adamberg, K., Nahku, R., Lahtvee, P.-J., Arike, L., and Vilu, R. (2010). Systems Biology Approach Reveals that Overflow Metabolism of Acetate in *Escherichia coli* Is Triggered by Carbon Catabolite Repression of Acetyl-CoA Synthetase. *BMC Syst. Biol.* 4, 1–13. doi:10.1186/1752-0509-4-166
- Valgepea, K., Adamberg, K., Seiman, A., and Vilu, R. (2013). *Escherichia coli* Achieves Faster Growth by Increasing Catalytic and Translation Rates of Proteins. *Mol. Biosyst.* 9 (9), 2344–2358. doi:10.1039/c3mb70119k
- Valgepea, K., de Souza Pinto Lemgruber, R., Abdalla, T., Binos, S., Takemori, N., Takemori, A., et al. (2018). H₂ Drives Metabolic Rearrangements in Gas-Fermenting *Clostridium autoethanogenum*. *Biotechnol. Biofuels.* 11 (1), 55. doi:10.1186/s13068-018-1052-9
- Valgepea, K., de Souza Pinto Lemgruber, R., Meaghan, K., Palfreyman, R. W., Abdalla, T., Heijstra, B. D., et al. (2017a). Maintenance of ATP Homeostasis Triggers Metabolic Shifts in Gas-Fermenting Acetogens. *Cel Syst.* 4 (5), 505–515. e5. doi:10.1016/j.cels.2017.04.008
- Valgepea, K., Loi, K. Q., Behrendorff, J. B., Lemgruber, R. d. S. P., Plan, M., Hodson, M. P., et al. (2017b). Arginine Deiminase Pathway Provides ATP and Boosts Growth of the Gas-Fermenting Acetogen *Clostridium autoethanogenum*. *Metab. Eng.* 41, 202–211. doi:10.1016/j.ymben.2017.04.007
- Valgepea, K., Talbo, G., Takemori, N., Takemori, A., Ludwig, C., Mueller, A. P., et al. (2021). Absolute Proteome Quantification in the Gas-Fermenting Acetogen *Clostridium autoethanogenum*. doi:10.1101/2021.05.11.443690
- Van Hoek, P., Van Dijken, J. P., and Pronk, J. T. (1998). Effect of Specific Growth Rate on Fermentative Capacity of Baker's Yeast. *Appl. Environ. Microbiol.* 64 (11), 4226–4233. doi:10.1128/aem.64.11.4226-4233.1998
- Wang, S., Huang, H., Kahnt, J., Mueller, A. P., Köpke, M., and Thauer, R. K. (2013). NADP-specific Electron-Bifurcating [FeFe]-Hydrogenase in a Functional Complex with Formate Dehydrogenase in *Clostridium autoethanogenum* Grown on CO. *J. Bacteriol.* 195 (19), 4373–4386. doi:10.1128/JB.00678-13
- Wilkins, M. R., and Atiyeh, H. K. (2011). Microbial Production of Ethanol from Carbon Monoxide. *Curr. Opin. Biotechnol.* 22 (3), 326–330. doi:10.1016/j.copbio.2011.03.005
- Wood, H. G. (1991). Life with CO or CO₂ and H₂ as a Source of Carbon and Energy. *FASEB j.* 5 (2), 156–163. doi:10.1096/fasebj.5.2.1900793
- Xu, H., Liang, C., Yuan, Z., Xu, J., Hua, Q., and Guo, Y. (2017). A Study of CO/syngas Bioconversion by *Clostridium autoethanogenum* with a Flexible Gas-Cultivation System. *Enzyme Microb. Technology* 101, 24–29. doi:10.1016/j.enzmictec.2017.03.002

Conflict of Interest: LanzaTech has interest in commercial gas fermentation with *C. autoethanogenum*. AH and MK are employees of LanzaTech.

The remaining authors declare that the research was conducted in the absence of any commercial or financial relationships that could be construed as a potential conflict of interest.

Publisher's Note: All claims expressed in this article are solely those of the authors and do not necessarily represent those of their affiliated organizations, or those of the publisher, the editors and the reviewers. Any product that may be evaluated in this article, or claim that may be made by its manufacturer, is not guaranteed or endorsed by the publisher.

Copyright © 2022 de Lima, Ingelman, Brahmabhatt, Reinmets, Barry, Harris, Marcellin, Köpke and Valgepea. This is an open-access article distributed under the terms of the Creative Commons Attribution License (CC BY). The use, distribution or reproduction in other forums is permitted, provided the original author(s) and the copyright owner(s) are credited and that the original publication in this journal is cited, in accordance with accepted academic practice. No use, distribution or reproduction is permitted which does not comply with these terms.